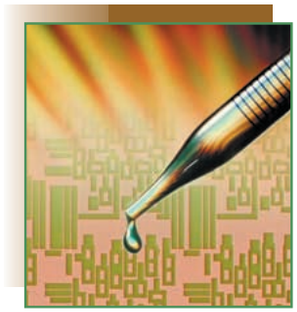

Streaming Dielectrophoresis for Continuous-Flow Microfluidic Devices

A Particle Filter/Concentrator That Works by Competing Electrokinesis and Dielectrophoresis

ERIC B. CUMMINGS

Electrokinesis (EK) and dielectrophoresis (DEP) are two technologically important transport phenomena produced by applying an electrostatic field to a conductive fluid. EK was first observed by Reuss [1] in 1809 and has been studied extensively since the 19th century. DEP has been studied since the seminal papers and book [2] of Pohl in the 1970s. The current push to develop microfabricated chemical and biological processing and analysis systems has renewed interest in these phenomena. DEP has been used for manipulating, fusing, sorting, and lysing biological cells and particles [3]–[5].

This article describes the engineering development of a 160× continuous-flow, selective particle filter/concentrator that works by a competition between DEP and EK in a microfluidic circuit. Filtration and concentration are common sample-processing steps since raw clinical and environmental samples typically contain background particles that must be removed and target particles are relatively dilute. For example, to test for dangerous levels of bacteria in water samples, one must be able to detect a single live bacterium in a liter of water. One must further be able to reject the vast preponderance of background and dead bacteria in the sample or risk overwhelming downstream analytical systems. Aerosol samples collected into water have somewhat lower volumetric requirements (e.g., 5 ml) but similar requirements for selectivity. Clinical samples like whole blood contain a high-conductivity liquid and a very high concentration of cells and intercellular macromolecules and aggregates. No single microfluidic filter/concentrator design can cover the range of required flow rates, conductivities, and target particle sizes. Rather, a rational design methodology supports customizing devices to perform specific functions robustly and effectively.

Developing this class of filter/concentrators illuminates a number of design issues that are critical to achieving good selectivity. It also demonstrates methods of improving system robustness, e.g., insensitivity to fouling, and shows the engineering costs of these methods, e.g., decreased electrical efficiency and increased fluid heating. This development especially shows how one can apply numerical simulations, theory, and experimental observation to microfluidic design.

Analysis, simulation, operation, validation, fabrication, and function are all subject to engineering compromises in this design methodology. The central compromise of the family of designs is the restriction that devices internally contain only insulators and that fluids and all interior surfaces are uniform [6]. This restriction in operation is made to allow the flow to be analyzed and simulated easily. Coincidentally, it also improves performance and function by ensuring devices produce the least hydrodynamic dispersion and do not electrochemically alter the liquid or generate bubbles. (It is interesting that compromises made to simplify theory often point to an operational ideal, e.g., minimum dispersion, minimum power, etc., and have value apart from making a problem mathematically tractable.) This restriction simplifies fabrication over alternative approaches that embed electrodes [7]–[9], improving the chances for mass producibility and ultimately marketability. While a designer may elect to relax this restriction, for this exercise, the design is constrained to two dimensions.

Electrokinesis

When an electric field is applied across a fluid, charged particles migrate along electric-field lines. This process is called *electromigration* or *electrophoresis*. As the particles move, they collide with other particles, transferring both momentum and energy to the rest of the fluid. If the fluid has no net charge, the momentum transferred by positively charged particles just cancels the momentum from negatively charged particles, and the transferred energy appears as random thermal motion, or heat, a process called *Joule heating*.

The interior of homogeneous liquids generally is *electroneutral,* or contains no appreciable net charge. Any imposed or spontaneous charge imbalance produces an electric field that rapidly conducts the imbalance away.

However, a net electric charge spontaneously and stably appears at most liquid interfaces with either gases, liquids, or solids. Like other surface phenomena such as surface tension, this net charge arises as the system minimizes its internal energy. Of particular interest is the interface between water and glass or silica, in which the internal energy is minimized by a chemical reaction that dissociates the water and covalently binds negatively charged hydroxyl ions (OH^-) to the surface, immobilizing a net negative charge there. The negative charge attracts positive ions in the water to the walls and repels negative ions from the walls, inducing an equal and opposite net charge in the liquid in the immediate vicinity of the wall. Together, these opposing charged regions are called the *electric double layer* (EDL).

The charge separation in the EDL produces an *intrinsic electric field* normal to the interface that decays with distance from the interface as the charges equilibrate under electrical forces and thermal collisions. The characteristic length of this decay is called the *Debye length* and is typically in the 1–100-nm range. A fraction of the liquid-borne charge is immobilized by the high intrinsic electric field (as high as ~10^9 V/m) nearest the wall, but the rest is free to move. Thus, when an electric field is applied, these interfacial charges electromigrate. Since the fluid is not electrically neutral, these charges can transfer a net momentum to the fluid within the EDL. This momentum transfers to the rest of the fluid by viscous diffusion, producing a fluid flow called *electroosmosis*.

Both electrophoresis and electroosmosis are linear in the applied electric field, in that doubling the electric field doubles the flow velocity. While these phenomena are actually physically identical, semantically they differ in their frame of reference: electrophoresis describes the motion of a charged object relative to a fixed immersion fluid while electroosmosis describes the motion of the immersion fluid relative to a fixed charged object.

The electrophoretic velocity $\mathbf{u}_{EP}$ of a particle with respect to its immersion liquid is proportional to the applied electric field $\mathbf{E}$ by an *electrophoretic mobility* μ_{EP} that is characteristic of the particle and liquid. The average velocity of an immersion liquid relative to a flow channel wall $\mathbf{u}_{EO}$ can be similarly related to the applied field by an *electroosmotic mobility* μ_{EO} that is characteristic of the liquid and channel material. For uniform, conductive liquids in uniform insulating, impermeable flow channels that are much larger than the Debye length, the flow velocity is everywhere proportional to the local applied electric field through this mobility, not just in an average sense [10]. This special flow is called *ideal electroosmosis* and is of considerable practical interest since it is simple to analyze and can produce less hydrodynamic dispersion than any other flow.

Generally, one actually observes and utilizes EK, the net motion of particles that occurs through both electrophoresis and electroosmosis, $\mathbf{u}_{EK} = \mathbf{u}_{EP} - \mathbf{u}_{EO}$. The average particle motion is related to the applied electric field by

$$\mathbf{u}_{EK} = \mu_{EK}\,\mathbf{E}, \tag{1}$$

where μ_{EK} is an *electrokinetic mobility* that is characteristic of the system of particle, liquid, and channel material. The direction and magnitude of the electrokinetic flow of a particle thus depends on the composition and interactions of these three elements. While a variety of theoretical relations exist to relate the EK mobility approximately to physical and chemical properties of this system, this mobility can be regarded for design purposes as an empirical system property.

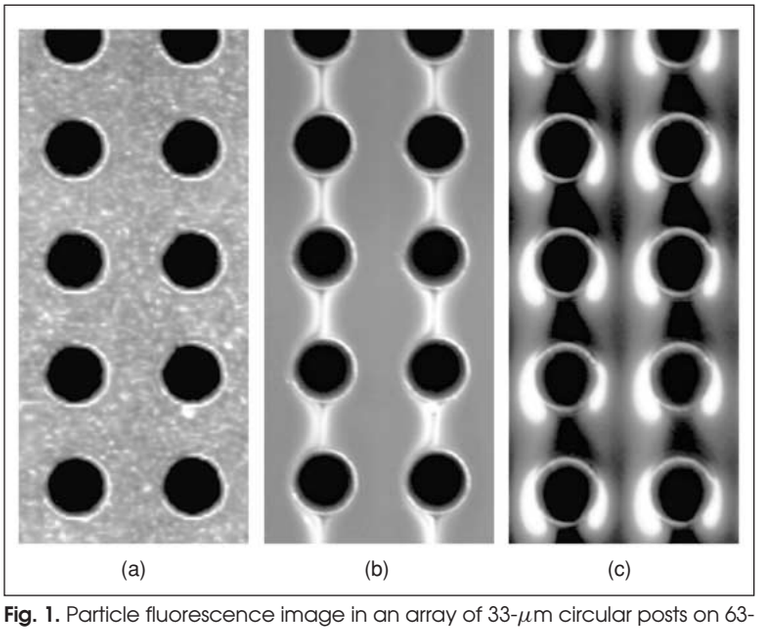

Fig. 1. Particle fluorescence image in an array of 33-μm circular posts on 63-μm centers. (a) Ideal electrokinesis, (b) streaming dielectrophoresis, and (c) trapping dielectrophoresis of fluorescent 200-nm polystyrene microspheres. The flow is from top to bottom produced by applied fields of ~1 V/mm, ~25 V/mm, and ~100 V/mm, respectively.

The concept of ideal electroosmosis can be extended to *ideal electrokinesis,* provided the particles are dilute and small compared to the channel geometry so that they do not appreciably influence the flow field [6]. Interestingly, ideal electrokinetic flows cannot concentrate or rarefy particles, so ideal electrokinesis alone cannot be used to make particle filters or concentrators. Electrokinetic devices can concentrate and filter particles by intentionally violating the conditions for ideality. For example, electrokinetic traps contain permeable surfaces; sample stacking and isotachophoretic devices concentrate by the use of nonuniform liquids. The filter/concentrator devices under consideration here use ideal electrokinetic flows to convey particles and liquids with low dispersion and to compete with another transport mechanism that is able to concentrate and rarefy particles: dielectrophoresis.

Dielectrophoresis

When an electric field is imposed across an immersed particle, the particle and immersion liquid polarize and conduct by a variety of mechanisms that are characteristic of the particle and liquid [2]. The particle and the immersion liquid

are each characterized by a complex conductivity, $\tilde{\sigma}(\omega) \equiv \sigma(\omega) + i\omega\alpha(\omega)$, where σ is the real conductivity, α is the polarizability, and ω is the angular frequency of the electric field. Because these electrical properties generally vary with frequency, this dependence is noted explicitly. A complex polarizability is often used instead of the conductivity to describe a material's response to an electric field, but this description unfortunately introduces a singularity at zero frequency (dc).

The theory of electrostatics shows that the potential energy of a material having a finite complex conductivity decreases with increasing electric field intensity. Thus, both mobile particles and immersion liquid experience a force toward regions of high electric field intensity. The motion produced by this force is called DEP. The material having the greatest complex conductance experiences the greatest dielectrophoretic force and thus displaces or buoys the lower-conductivity materials from the high-field regions. The motion of a particle toward high-field regions is called *positive DEP* and the motion of the particle away from high-field regions under this dielectrophoretic buoyancy force is called *negative DEP*. For particles that lack an intrinsic dipole moment, like most, DEP is initially quadratic in the applied electric field. Thus, when the applied field doubles, the dielectrophoretic velocity quadruples. Again, the dielectrophoretic velocity $\mathbf{u}_{DEP}$ of an immersed particle can be related to the

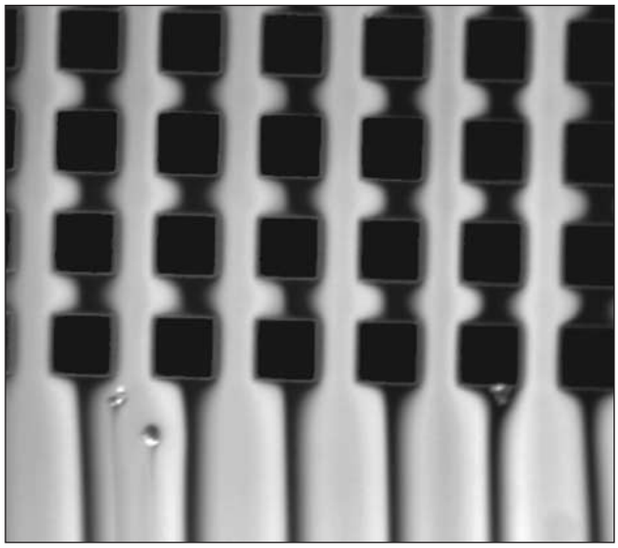

Fig. 2. Particle fluorescence image of streamimg dielectrophoresis at the end of an array. The flow is from top to bottom produced by an applied field of ~80 V/mm, oriented at ~2° with respect to columns of 36–μm square posts on 63–μm centers. Particles are significantly depleted from the regions along the post columns.

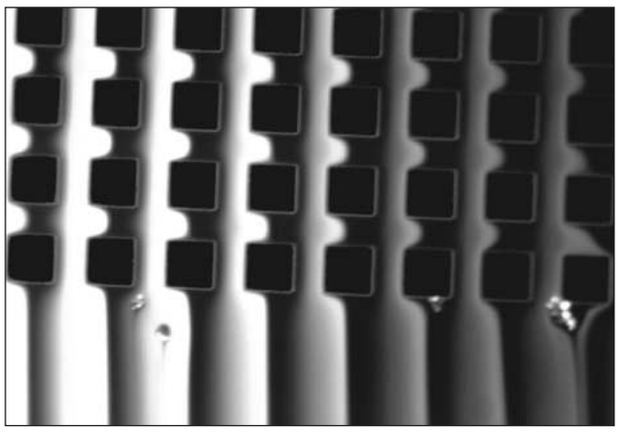

Fig. 3. Particle fluorescence image of depletion at the end of an array tilted by ~3° with respect to the mean flow. Particles are removed from the electrokinetic flow between the posts, concentrating on the left side of each column. The concentration gradient across the array shows the cumulative effect of depletion along the 56-row array.

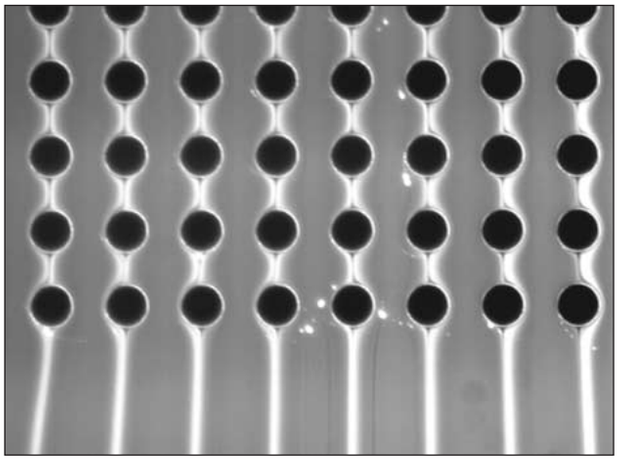

Fig. 4 Particle fluorescence image of streaming dielectrophoresis at the end of an array. The flow is from top to bottom produced by an applied field of ~25 V/mm oriented down columns of 33–μm circular posts on 63–μm centers. The fluorescence intensity variation shows the dielectrophoretic concentration of particles in the region along the post columns.

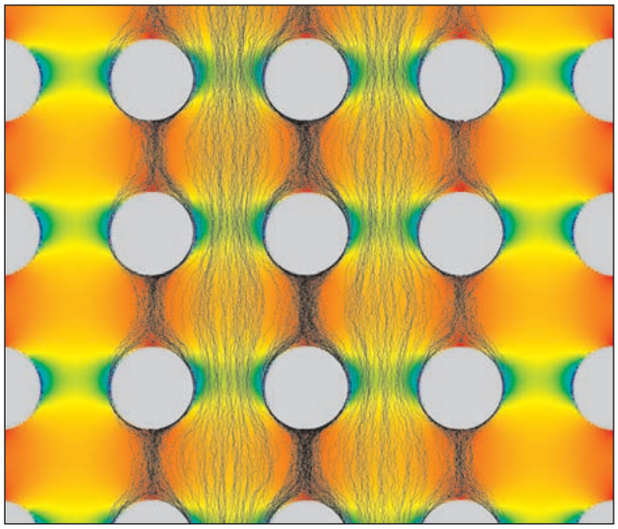

Fig. 5. Continuum and particle simulation of combined electrokinesis, dielectrophoresis, and diffusion in an array of circular posts showing particle concentration along the posts. The background color depicts the mean particle speed: red and blue are zero and the highest speed, respectively.

Simulation-assisted engineering bridges the gulf between experimental and numerical observation of streaming DEP and the design of a practical particle concentrator.

electric field by a *dielectrophoretic mobility* μ_{DEP}, but the relationship is more complicated than for EK,

$$\mathbf{u}_{DEP} = -\mu_{DEP}(\omega)\,\nabla\,[\mathbf{E}(\omega)\cdot\mathbf{E}(\omega)], \qquad (2)$$

for a single-frequency electric field $\mathbf{E}$ because a particle's dielectrophoretic potential energy is proportional to the local electric field intensity. Again, this mobility can be related theoretically to the physical and chemical properties of the particles and liquids in the system, but for design purposes, the dielectrophoretic mobility can be regarded as an empirical system property.

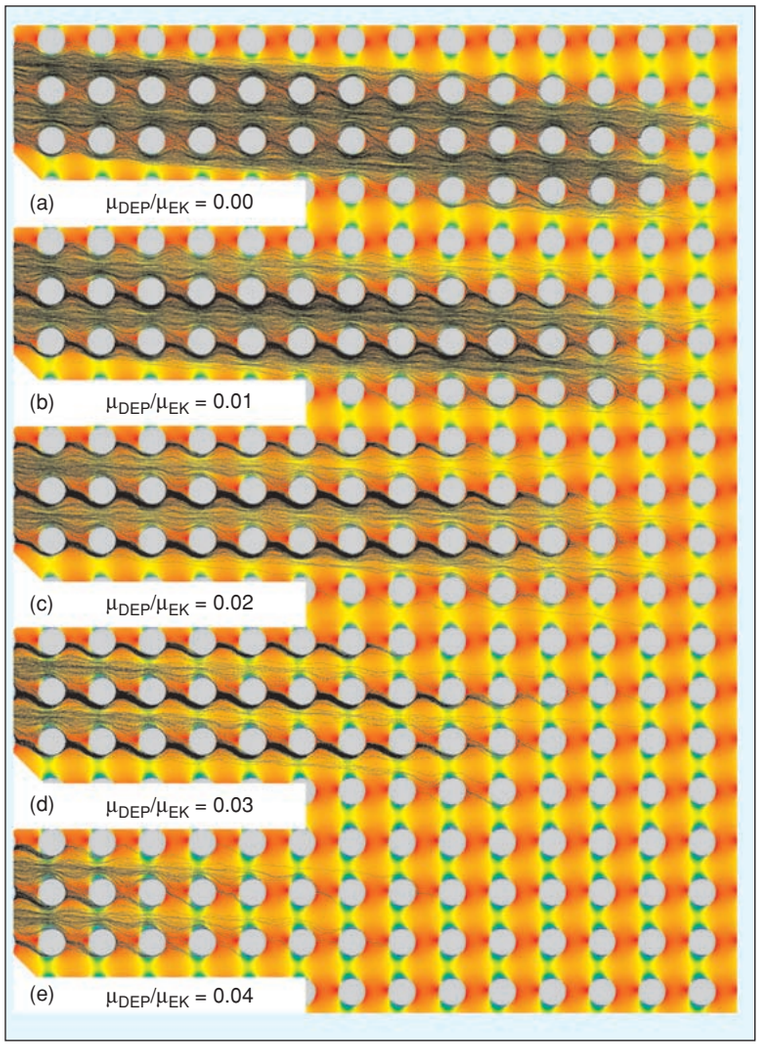

Fig. 6. Continuum and particle simulation of combined electrokinesis, dielectrophoresis, and diffusion in an array of circular posts at ~15° incidence showing enhancement-mode particle concentration. The background color depicts the mean particle speed: red and blue are zero and the highest speed, respectively. Dielectrophoretic trapping occurs for particles having high DEP mobility. The images at right show the combined EK and DEP isopotentials within a cell of the array.

The spatial gradient in (2) shows that dielectrophoresis requires a nonuniform electric field. Conventionally, the electric-field nonuniformity is produced by embedding spatially nonuniform arrangements of electrodes into the flow channel. At sufficiently small electrode spacing, large electric field gradients can be produced from low-voltage excitations, the kind that conventional audio- and radio-frequency electrical instruments generate. However, these electrodes electrochemically alter the fluid, generate unwanted electrolysis bubbles, polarize in a complicated manner, are susceptible to fouling, and generally require nontrivial fabrication processes. Embedded electrodes also violate the conditions for ideal electrokinesis, significantly complicating the method of solution for the flow field within the devices. Moreover, virtually all arrangements of such electrodes do not allow electrokinetic conveyance, so particles are usually conveyed using highly dispersive *advection* (pressure-driven flow).

A spatially nonuniform channel geometry produces a nonuniform electric field that can drive dielectrophoresis [11] in a manner that is compatible with ideal electrokinetic conveyance [6]. Constricting, expanding, or placing obstacles like insulating posts in microchannels creates engineerable electric-field gradients that facilitate dielectrophoretic devices in which the electric field is applied by remote electrodes. Remote electrodes minimally perturb the flow in the system: no electrochemical reactions occur in the channels. Such devices can be microfabricated by simple techniques such as glass etching or mass-fabricated by plastic stamping and embossing. Importantly, the devices are amenable to analysis and thus can be designed and optimized rationally. The downside to the use of remote electrodes is the need to apply higher voltages (e.g., 100s to 1,000s of volts) to produce a desired electric field gradient, necessitating the use of custom or nonstandard electric waveform generators and supplies, a comparatively minor concession.

A spatially nonuniform channel geometry produces a nonuniform electric field that can drive dielectrophoresis in a manner that is compatible with ideal electrokinetic conveyance.

Streaming Dielectrophoresis

Three different flow regimes typically exist for flows in which dielectrophoresis is combined with electrokinesis [6]. Because of its second-order dependence on the applied electric field, DEP is practically absent at low applied fields (e.g., ~1 V/mm) so this flow regime is simply called *electrokinesis*. As Figure 1(a) shows, ideal electrokinesis neither concentrates nor rarefies particles.

Above a threshold applied electric field called the *DEP trapping threshold,* DEP overcomes EK in appreciable regions of the flow, called *DEP traps,* where particles entering the system become immobilized, as Figure 1(c) shows. The value of this threshold field depends linearly on the ratio of the electrokinetic and dielectrophoretic particle mobilities and the length scale of geometrical field-concentrating structures. The flow regime in which traps appear is called *trapping DEP*. Trapping DEP is of considerable interest for *trap-and-release* particle concentration, in which a high electric field is applied for a time to collect particles into the traps and a lower electric field is used to elute or release the particles.

At fields just below the DEP trapping threshold, DEP is unable to immobilize particles against the electrokinetic conveyance but is able to shuffle particles around the flow. In this flow regime, particles concentrate and rarefy into flowing filamentary streams, as Figure 1(b) shows. This flow regime, called *streaming DEP,* is used here for continuous-flow particle concentration. The nature of streaming dielectrophoretic flow in arrays depends sensitively on post shapes and orientation of the array with respect to the applied electric field, making such a system subject to engineering optimizations.

Depletion and Enhancement

Figure 2 shows highly rarefied filaments flowing down columns of posts. The large stagnation regions above and below the posts are DEP potential barriers for particles having a positive DEP mobility. The long residence times of the flow between the posts allows this barrier to repel particles in an effect called *depletion,* wherein the concentration of particles is significantly reduced along columns. This depletion effect persists at modest flow angles with respect to the array.

Figure 3 shows depletion at a mean flow angle of ~3° with respect to the posts. The effect of depletion in this image is the complete removal of particles from the flow that passed between the posts and the significant concentration of particles held back by the DEP barriers. This effect and this geometry are employed to create the particle filter/concentrator.

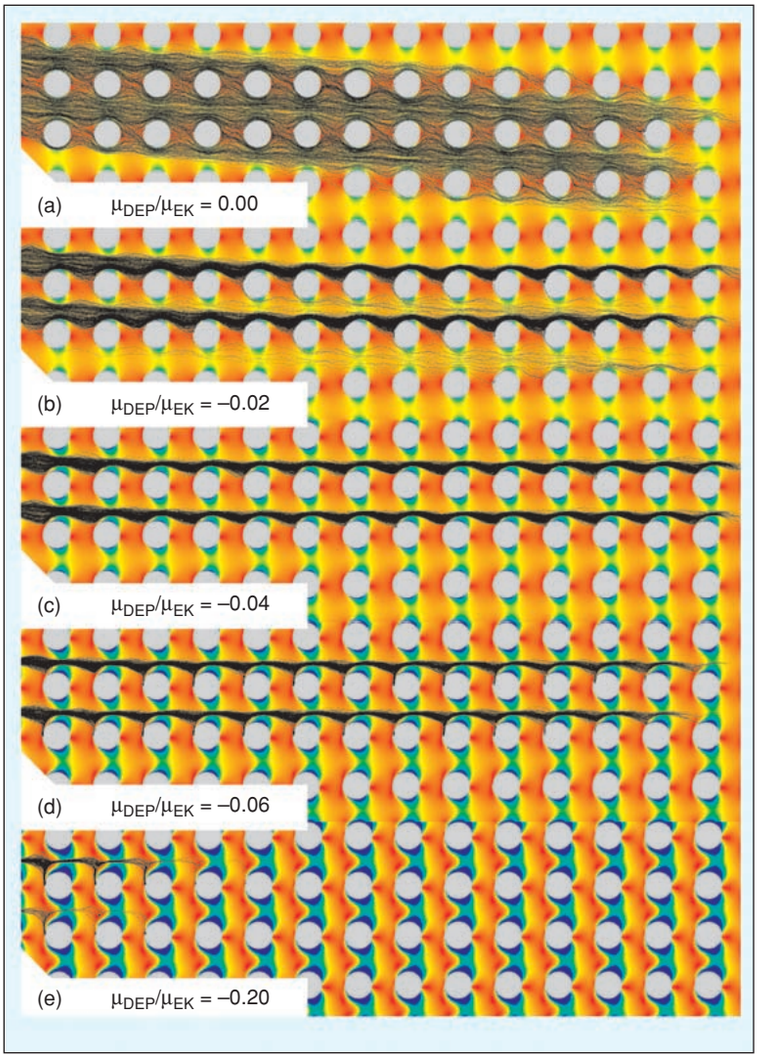

Fig. 7. Simulation similar to that in Figure 6 for particles having negative dielectrophoretic mobility showing depletion-mode particle concentration. Particle concentration occurs at the opposite side of the posts from that in Figure 6. Dielectrophoretic trapping occurs for particles having a large negative DEP mobility. The images at right show the combined EK and DEP isopotentials within a cell of the array.

The choice of ideal electrokinesis, the simplest possible flow, to convey particles makes such simulations and geometrical optimizations tractable—and gives intuition a needed boost.

The nature of the dielectrophoretic filaments is sensitive to post shape as well as array angle. Figure 4 shows the streaming flow at the end of an array of circular posts. In this flow, apart from a slight rarefaction immediately near the stagnation streamline down the centerline of the posts, particles are concentrated along rows of posts, an effect called *enhancement*. Figure 5 shows the enhancement effect in a particle simulation of combined electrokinesis, dielectrophoresis, and diffusion in a similar array of circular posts at 0° incidence. Like the observed depletion function of the columns of square posts, the enhancement function of the circular posts can be utilized to filter or concentrate particles.

Figure 6 shows numerical simulations of enhancement-mode concentration for particles having different positive dielectrophoretic mobilities. At zero DEP mobility, particles follow the electrokinetic flow at ~15° down from the left to the right. Particles having a sufficiently high DEP mobility overcome the downward electrokinetic motion to flow along the columns of posts. Above a threshold mobility that decreases with applied electric field, particles become trapped at the field concentrations at the sides of the posts. The simulation is linear in that it does not account for finite particle size or perturbations to the flow produced by the presence of the particles. Some particles are prematurely trapped at the sides of posts as a result of field concentration artifacts from gridding the post boundary. This trapping portends a similar effect that can occur from surface roughness of the posts.

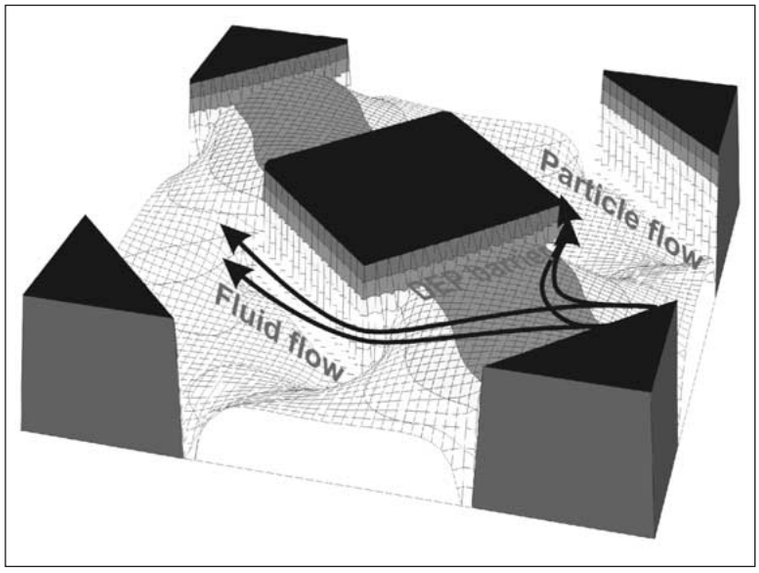

Fig. 8. Electrostatic potential surface experienced by particles passing through a cell of the array. The potential barrier between the posts strips particles from the mean flow.

An array that functions in enhancement mode for particles having a positive DEP mobility will function in depletion mode for particles having a negative DEP mobility. Figure 7 shows simulations similar to those in Figure 6 but for particles having a negative DEP mobility. Note that the particles concentrate on the opposite side of the columns. Again, trapping occurs at sufficiently high DEP mobility. The relative thresholds of the enhancement and depletion effects depend on the post shape. For circular posts, the threshold for negative DEP depletion is about twice that for positive DEP enhancement.

Engineering a Streaming DEP Particle Concentrator

Simulation-assisted engineering bridges the gulf between experimental and numerical observation of streaming DEP and the design of a practical particle concentrator. The resulting concentrator is a patterned-insulator microdevice that employs streaming DEP to concentrate selected particles by a factor of 160 from a continuous flow. To facilitate embedding in planar microsystems, the device is constrained to two dimensions and binary channel depths: zero (insulator) and unity (channel). The device is based upon the observation in experiment and simulation that selected particles follow columns of the post arrays even when there is a small tilt angle of the array with the mean flow. By tilting the array toward one side of the channel, particles having a range of dielectrophoretic mobilities concentrate at the channel side during passage through the system. Arrays that work in either depletion- or enhancement-mode be used in such a device. The device that is developed in this section operates in depletion-mode for particles having a positive DEP mobility. While such a system can benefit from a number of optimizations of post size, shape, and spacing, the emphasis in this discussion is on generic engineering issues that arise when designing these systems, particularly issues that can be addressed through theory and simulation—before committing a design to a costly prototyping run.

Figure 8 shows the electrostatic potential surface encountered by particles traversing a cell of an array like that in Figure 3. The flow is from top to bottom. The dielectrophoretic potential barrier strips particles from the near-stagnant regions between the posts, so particles concentrate along the upstream side of the column. Figure 9 shows a simulation of the dielectrophoretic potential in an abbreviated array of posts. Red regions are potential barriers. The particles flow down the post columns while the flow follows the wall boundaries, producing a

spatial separation. By stacking multiple copies of this array, all particles whose mobility is greater than a threshold value and less than the trapping threshold will be stripped from the main flow and appear highly concentrated at the right side of the bottom of the array.

Design Details

The conversion of a conceptual design into working hardware involves a detail design step on which the performance and possibly success of the hardware hinges. Analysis and simulation have assisted both the conceptual and detail design of this dielectrophoretic concentrator. Performance metrics of this design are the absence of undesired trapping sites where blockages can start, the insensitivity to clogging, and the sharpness in the threshold DEP mobility of the concentrator. This sharpness is maximized when all the DEP potential barriers in the filter have the same shape and height, a condition achieved in the interior of a uniform infinite array of uniform posts. The interior of the DEP filter/concentrator is therefore designed to appear to the flow as though the array of posts repeats infinitely in the plane of the device, i.e., by

- contouring the side walls of the device to the mean-flow streamlines in a uniform infinite array of the desired posts at the desired flow-tilt angle with respect to the applied field
- tilting the array-filled flow channel with respect to the open entry and exit ports to ensure the electric field is applied evenly across the tilted array
- patterning the walls at the entry and exit ports of the device to match free streamlines emerging from a semi-infinite array at the channel-tilt angle specified
- modifying the shape of the posts at the entry and exit rows of the array to prevent excessive field concentrations at the interfaces between the open- and patterned-channel sections.

These design details are illustrated in Figure 10. The inset at right shows a detail of the wall contouring. The flow-tilt angle has been adjusted so that the streamline patterns repeat after the passage of an integer multiple n of rows of posts. In the example shown, $n = 8$. Generally, n is sufficiently large (e.g., ≥8) to produce the requisite DEP potential barriers between the posts. The parameter n need not be integral for the device to operate, but the details of the wall contouring become more complicated than in this example. The side walls for the full array (at left) are constructed by stacking copies of this eight-row pattern. By symmetry, the left wall is the same as the right wall rotated by 180 degrees. The array-filled flow channel is tilted with respect to the entry and exit ports to obtain a uniform electric field across the array.

The transition from open channel to tilted array appears to the electrical flow as an abrupt conductance change across a tilted straight interface. For the electric field to be constant along this interface, the flow-incidence angle of the interface must satisfy the compatibility relation [12]

$$\tan(\theta_i)/\sigma_i = \tan(\theta_a)/\sigma_a, \qquad (3)$$

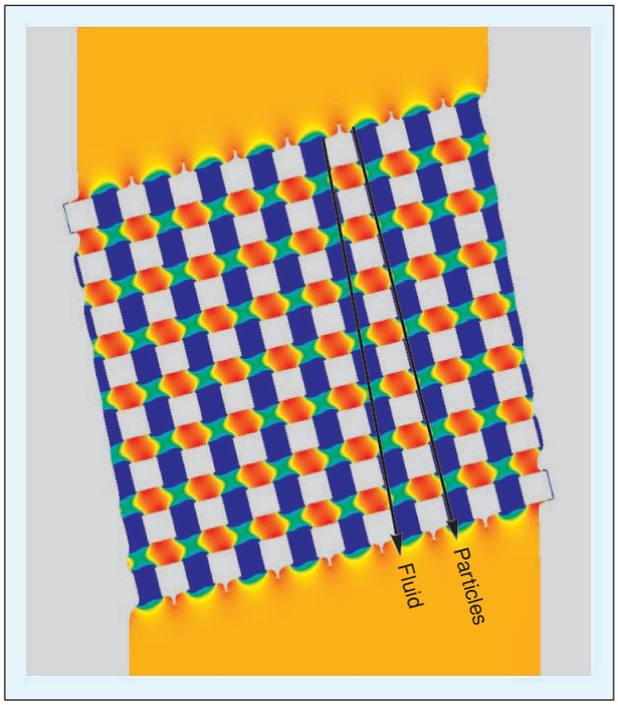

Fig. 9. Numerical simulation of the DEP potential within a truncated filter/concentrator array. The fluid flow follows the channel walls while the DEP barriers (red) redirect particles to follow array columns, producing a spatial separation.

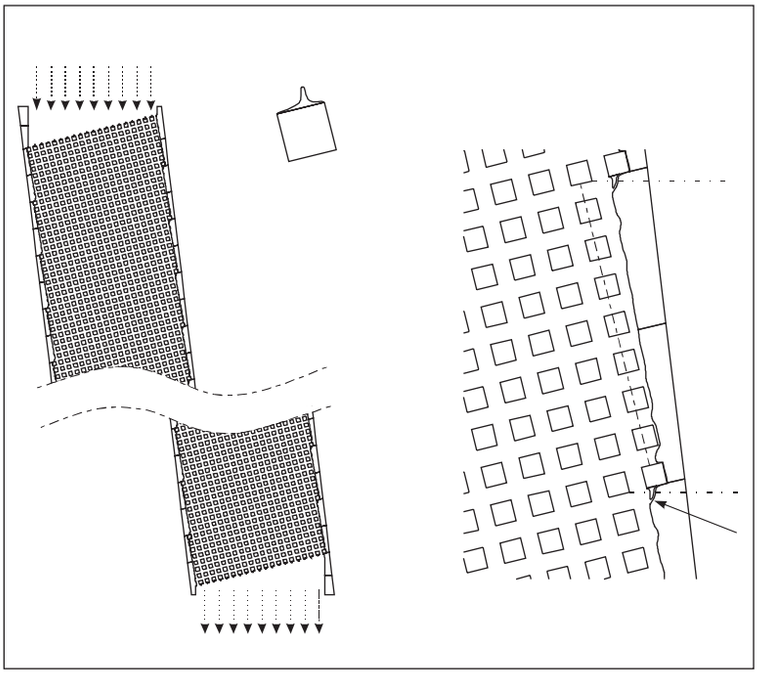

Fig. 10. Details of the dielectrophoretic filter/concentrator design. Left: tilted array channel; middle: tippet on posts on the entry and exit rows; right: repeated wall contouring and "spillway" modification (near the arrow). All particles within the dashed line pass through the narrow port indicated by the arrow.

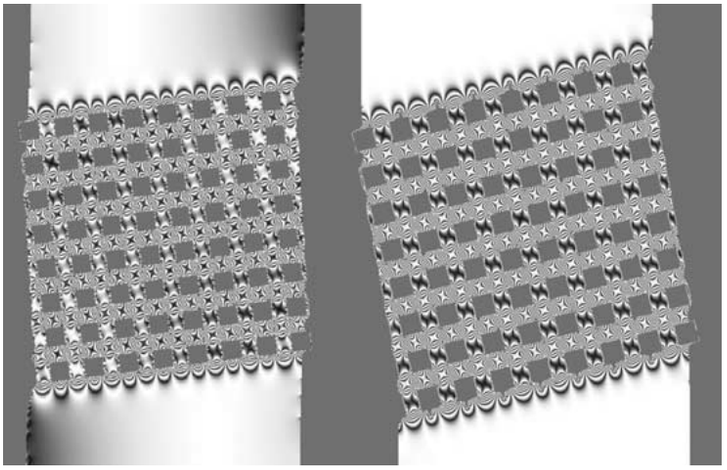

Fig. 11. Speed-field simulations of flow in a truncated section of the filter/concentrator. (a) The entry and exit ports are parallel to the array side walls, not satisfying compatibility (3), so the applied field is nonuniform across the entry and exit ports. (b) The side walls and array are tilted to satisfy compatibility so the applied field is uniform and the speed field is essentially identical in every cell of the array.

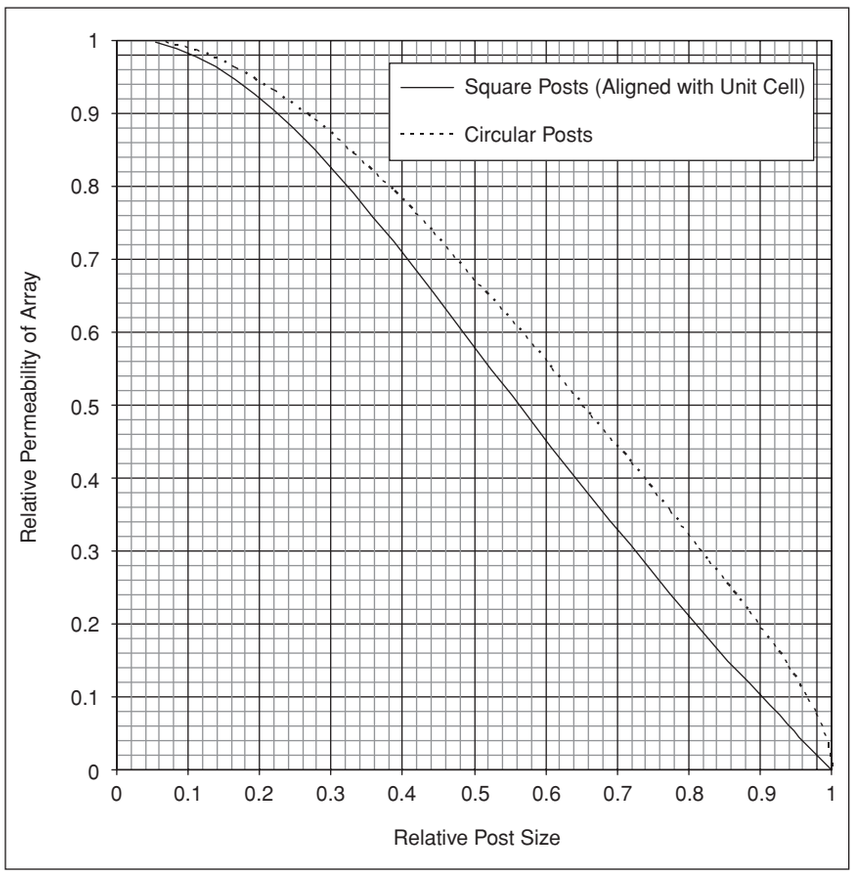

Fig. 12. Plot of the effective conductivity—the ratio of flux to applied voltage normalized to an open channel—of square arrays of square and circular posts versus the ratio of the post size to the post spacing.

where θ is the angle of the flow with respect to the normal to the interface, σ is the effective channel conductance per unit width, and the subscripts "i" and "a" respectively refer to the incident and array flows. Figure 11(a) shows a simulation of flow in a tilted-array design that does not satisfy this compatibility condition. The speed field is shown as a simulated interferogram in which the fringes correspond to speed contours. The dark fringe across the entry and exit ports shows a 10% variation in the applied field. This field persists through the array, as the variation in the cell–cell speed-field patterns show. Figure 11(b) shows a simulation of the same array design tilted to satisfy the compatibility condition (3). The electric field is uniform across the entrance and exit of the array. The speed fields in each cell are matched to <0.1%, apparently the limit set by the numerical discretization used in the simulation.

The effective conductance of the array is defined as the ratio of the total current through the array to the applied electric field and is a function of post shape and size. For a post having symmetry of rotation through 90°, the effective conductance does not depend on the flow angle through the array. Figure 12 shows a plot of the effective conductance relative to that of an open channel (σ_i/σ_a) of square arrays of circular and square posts (edges aligned with rows and columns) versus post size, obtained by numerical simulation. For general post shapes, the effective conductance is fixed by the choice of post and flow angle with respect to the columns of posts in the array θ_a, where $\tan\theta_a = 1/n$. Thus the choice of post and flow angle (or n) uniquely determines the incidence angle, θ_i, which appears in Figure 10 as a tilt of the straight outer boundary of the channel side walls, or equivalently as a horizontal offset between the entry and exit ports.

Finally, the electric field at the entry and exit rows of posts is somewhat higher than that experienced in the interior of the array. To prevent particles from being trapped on these rows, the shape of the post is modified slightly to reduce the field concentration. The "tippet" added to the top of the post, shown in the detailed inset in Figure 10, is an example of a shape modification that locally reduces this field concentration while having a negligible impact on the flow in the neighboring rows.

There are places where the array must *not* appear to be infinite. All particles whose DEP mobility is between the threshold of the filter and the threshold of trapping that are present in

the liquid between the dashed line and the wall pass through the orifice indicated by the arrow in Figure 10. Some alteration of either the post shape, wall contour, or a combination is needed in this region to weaken the DEP barrier so particles can spill through the orifice to the next set of rows. The panhandle-shaped post modifier immediately above the arrow in Figure 10 performs this function.

The filter concentration factor can be calculated geometrically by considering only the column of posts next to the wall. If the array is tilted so streamline patterns repeat every n rows, the fluid flux passing between each row is a fraction $1/n$ of the total flux through the column. All particles whose DEP mobility exceeds the threshold cross the columns through a single row at the wall. Thus the concentration factor per column is n. If there are m columns, and *at least* m sets of n rows in the array, the concentration factor is $m\,n$. For the array shown in Figure 10 this factor is 160 (8 times 20). Having more than m sets of n rows in the array does not increase the concentration factor but provides redundancy, which improves robustness against clogging and other imperfections at the cost of a loss in power efficiency and the need for higher voltages to apply the same electric field.

The complete design, ready to be placed on a photomask, is shown at 5–100× scale in Figure 13. Item 100 is the entry electrode; item 110 is an entry reservoir; item 120 is the entry channel. Item 130 is a side wall; item 140 is an array post; item 90 is the filter/concentrator channel. Items 150 and 155 are voltage waveform and pressure generators to produce the mean flow in the channel and drive dielectrophoresis. Item 160 is the particle harvesting port, item 180 is the particle concentrate reservoir, and item 200 is the concentrate electrode. Item 165 is the filtrate channel, item 170 is the filtrate reservoir, and item 190 is the filtrate electrode.

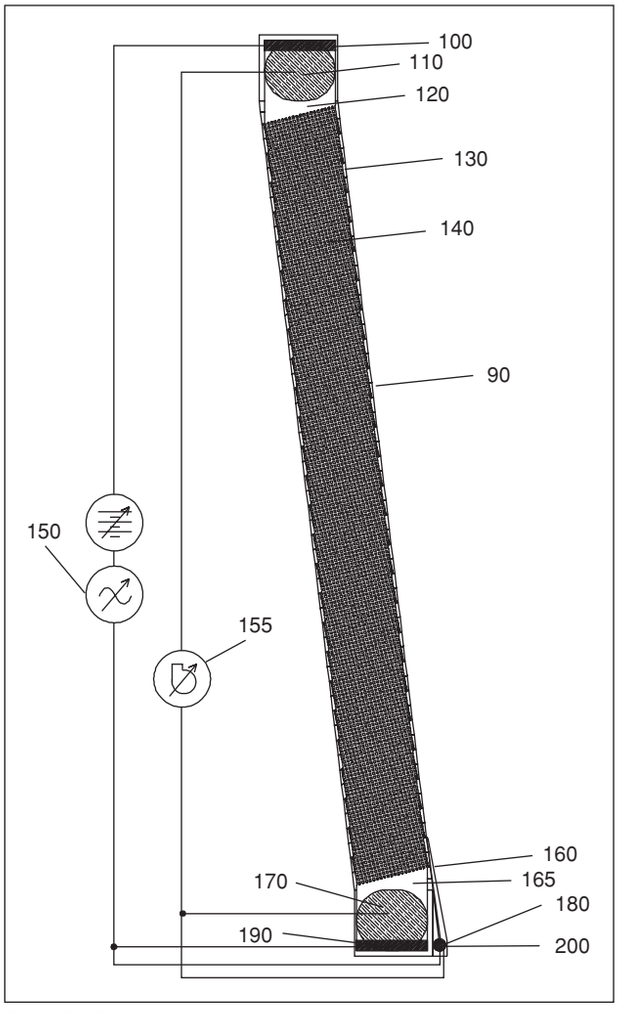

Fig. 13. Complete depletion-mode filamentary dielectrophoretic particle filter/concentrator design (5–100× depending on the size of the particles).

Conclusions

A broad range of devices can use ideal electrokinesis and dielectrophoresis in a variety of modes, as illustrated by the particular device shown in this article. Because these transport mechanisms are proportional to different powers of the electric field, the devices can be tuned at run time to select different classes of particles and even to switch flow regimes from streaming to trapping dielectrophoresis by varying the applied voltage. For example, trapping may be employed to hold the collected particles while a downstream device prepares for them. Since each microsystem has different requirements, rational design methodologies, grounded by theory and predictive models, become an important approach for synthesizing a design to specification rather than focusing solely on specific devices, keeping in mind that these methodologies only initially emerge through the experience of designing a variety of specific devices.

The function of these devices hinges on the detailed electric field distribution that resists intuition: designing by the seat-of-the-pants is a recipe for continued design/test/fabricate iterations. While they are no replacement for intuition and deep thought, modeling and simulation are critical for avoiding mistakes like unintentional particle traps and escapes, for developing design details like contoured walls, and ultimately for optimizing device performance. The choice of ideal electrokinesis, the simplest possible flow, to convey particles makes such simulations and geometrical optimizations tractable—and gives intuition a needed boost. Because this ideal represents a practically desirable limit, e.g., minimum-dispersion, the conditions for the validity of ideal electrokinesis can guide device and system design and fabrication. Of course clogging and the effects of highly concentrated particles complicate device operation in a stochastic and theoretically intractable way: there is no getting around flight-testing, but it is a good idea to start with a plane that at least flies *in theory*!

As observed experimentally and numerically, streaming dielectrophoresis is a novel flow regime for device development. It can be coherently reinforced within a patterned array to produce strong particle "depletion" and "enhancement," effects. This flow enables new classes of continuous-flow dielectrophoretic particle filter/concentrators and spectrometers. Given the need for rapid, automated, and miniaturized sample preparation, these devices will be a shot in the arm for medical sensors.

Acknowledgment

This work was supported by Sandia National Laboratories' Laboratory Directed Research and Development funding. Sandia is a multiprogram laboratory operated by Sandia Corporation, a Lockheed-Martin company, for the United

States Department of Energy under contract DE-AC04094AL85000.

Eric B. Cummings received a Ph.D. in aeronautics and chemistry from Caltech in 1995. He established the Applied Microfluidic Physics Laboratory at Sandia in 1997 and has worked extensively in the theory, diagnostics, and rational design of electrokinetic and dielectrophoretic microdevices. He has developed the theory of ideal electrokinesis, linear dielectrophoresis, and advanced particle-image velocimetry methodologies for microfluidics and stochastic flows and created a range of continuous and batch filter/concentrators for on-chip sample processing.

Address for Correspondence: Eric B. Cummings, Sandia National Laboratories, 7011 East Avenue, Livermore, CA 94550 USA. E-mail: ebcummi@sandia.gov.

References

[1] F.F. Reuss, Memoires de la Societe Imperiale de Naturalistes de Moscou, vol. 2. 1809, p. 327.
[2] H.A. Pohl, Dielectrophoresis, Cambridge, UK: Cambridge, 1978.
[3] R. Pethig, "Dielectrophoresis: Using inhomogeneous AC electrical fields to separate and manipulate cells," Crit. Rev. Biotechnol., vol. 16, 1996, pp. 331–348.
[4] P.R.C. Gascoyne and J. Vykoukal, "Particle separation by dielectrophoresis," Electrophoresis, vol. 23, pp. 1973–1983, 2002.
[5] M.P. Hughes, "Strategies for dielectrophoretic separation in laboratory-on-a-chip systems," Electrophoresis, vol. 23, pp. 2569–2582, 2002.
[6] E.B. Cummings and A.K. Singh, "Dielectrophoretic trapping without embedded electrodes," in Proc. SPIE Conf. Micromachining and Microfabrication, vol. 4177, 2000, pp. 164–173.
[7] G.H. Markx and R. Pethig, "Dielectrophoretic separation of cells: Continuous separation," Biotechnol. Bioeng., vol. 45, pp. 337–343, 1995.
[8] G.H. Markx, J. Rousselet, and R. Pethig, "DEP-FFF: Field-flow fractionation using non-uniform electric fields," J. Liquid Chrom. Rel. Tech., vol. 20, pp. 2857–2872, 1997.
[9] X.B. Wang, J. Yang, Y. Huang, J. Vykoukal, F.F. Becker, and P.R.C. Gascoyne, "Cell separation by dielectrophoretic field-flow-fractionation," Anal. Chem., vol. 72, pp. 832–839, 2000.
[10] E.B. Cummings, S.K. Griffiths, R.H. Nilson, and P.H. Paul, "Conditions for similitude between the fluid velocity and electric field in electroosmotic flow," Anal. Chem., vol. 72, pp. 2526–2532, 2000.
[11] C.F. Chou, J.O. Tegenfeldt, O. Bakajin, S.S. Chan, E.C. Cox, N. Darnton, T. Duke, and R.H. Austin, "Electrodeless dielectrophoresis of single- and double-stranded DNA," Biophysical J., vol. 83, pp. 2170–2179, 2002.
[12] G.J. Fiechtner and E.B. Cummings, "Faceted design of channels for low-dispersion electrokinetic channels for microfluidic systems," Anal. Chem, to be published.